

# 1 **High-Resolution Melt Curve Analysis: An Approach for Mutation** 2 **Detection in the TPO Gene of Congenital Hypothyroid Patients in** 3 **Bangladesh**

4  
5 Mst. Noorjahan Begum<sup>1,2,3</sup>, Rumana Mahtarin<sup>2</sup>, Md Tarikul Islam<sup>2</sup>, Nusrat Jahan Antora<sup>2</sup>,  
6 Suprovath Kumar Sarker<sup>2</sup>, Nusrat Sultana<sup>2</sup>, Abu A. Sajib<sup>1</sup>, Abul B.M.M.K Islam<sup>1</sup>, Hurjahan  
7 Banu<sup>4</sup>, M A Hasanat<sup>4</sup>, Kohinoor Jahan Shyamaly<sup>5</sup>, Suraiya Begum<sup>5</sup>, Tasnia Kawsar Konika<sup>6</sup>,  
8 Shahinur Haque<sup>6</sup>, Mizanul Hasan<sup>6</sup>, Sadia Sultana<sup>7</sup>, Taufiqur Rahman Bhuiyan<sup>8</sup>, Kaiissar  
9 Mannoor<sup>2</sup>, Firdausi Qadri<sup>2,8</sup>, Sharif Akhteruzzaman<sup>1\*</sup>

10  
11 <sup>1</sup>Department of Genetic Engineering & Biotechnology, University of Dhaka, Dhaka-1000,  
12 Bangladesh.

13 <sup>2</sup>Institute for Developing Science and Health Initiatives (ideSHi), ECB Chattar, Mirpur, Dhaka,  
14 Bangladesh.

15 <sup>3</sup>Virology Laboratory, Infectious Diseases Division, International Centre for Diarrhoeal Disease  
16 Research, Bangladesh, Mohakhali, Dhaka-1212, Bangladesh.

17 <sup>4</sup>Department of Endocrinology, Bangabandhu Sheikh Mujib Medical University (BSMMU),  
18 Shahbag, Dhaka-1000, Bangladesh.

19 <sup>5</sup>Department of Pediatrics, Bangabandhu Sheikh Mujib Medical University (BSMMU) Shahbag,  
20 Dhaka-1000, Bangladesh.

21 <sup>6</sup>Nuclear Medicine and Allied Sciences, Bangabandhu Sheikh Mujib Medical University  
22 (BSMMU), Shahbag, Dhaka-1000, Bangladesh.

23 <sup>7</sup>Scintigraphy Division, Bangabandhu Sheikh Mujib Medical University (BSMMU) Shahbag,  
24 Dhaka-1000, Bangladesh.

25 <sup>8</sup>Mucosal Immunology and Vaccinology, Infectious Diseases Division, International Centre for  
26 Diarrhoeal Disease Research, Bangladesh, Mohakhali, Dhaka-1212, Bangladesh.

27  
28 \*Correspondence: [sazaman@du.ac.bd](mailto:sazaman@du.ac.bd)

## 30 **Abstract**

31 Thyroid Peroxidase (*TPO*) is known to be the major gene involved in Congenital hypothyroid  
32 patients with thyroid dyshormonogenesis. This present study aimed to establish high-resolution  
33 melting (HRM) curve analysis as a supplementary mutation detection approach of Sanger  
34 sequencing targeting commonly found mutations c.1117G>T, c.1193G>C, and c.2173A>C in the  
35 *TPO* gene in Bangladeshi patients. We enrolled 36 confirmed cases of congenital hypothyroid  
36 patients with dyshormonogenesis to establish the HRM method. Blood samples were collected,  
37 and genomic DNA was isolated for molecular techniques. Among the 36 specimens, 20 were pre-  
38 sequenced, and mutations were characterized through Sanger sequencing. The pre-sequenced  
39 specimens (n=20) were then subjected to real-time PCR-HRM curve analysis to get the appropriate  
40 HRM condition capable of differentiating heterozygous and homozygous states for the three  
41 mutations from the wild-type state. Furthermore, 16 unknown specimens were subjected to HRM  
42 analysis to validate the method. This method showed 100 percent sensitivity and specificity to  
43 distinguish wild-type alleles from homozygous or heterozygous states (c.1117G>T, c.1193G>C,  
44 and c.2173A>C) of alleles commonly found in Bangladeshi patients. The HRM data was found to  
45 be similar to the sequencing result, thus confirming the validity of the HRM approach for *TPO*  
46 gene mutation.

47 In conclusion, the established HRM-based molecular technique targeting c.1117G>T, c.1193G>C,  
48 and c.2173A>C mutations could be used as a high throughput, rapid, reliable, and cost-effective  
49 screening approach for the detection of all common mutations in *TPO* gene in Bangladeshi patients  
50 with dyshormonogenesis.

51

52 **Key words:** Congenital Hypothyroidism, Thyroid Dyshormonogenesis, Thyroid Peroxidase,  
53 High-Resolution Melt Curve Analysis

54

## 55 **1. Introduction**

56 Congenital hypothyroidism (CH) is the endocrine disorder in which thyroid hormone deficiency  
57 occurs at birth and is the most common preventable cause of mental retardation [1-3]. This  
58 condition can lead to different clinical complications such as irreversible brain damage, delayed  
59 developmental milestones, lethargy, and slowdown of the body's overall metabolism of the  
60 patients if untreated. Early detection and initiation of treatment can reverse such complications [4].  
61 The CH frequency is 1 in 3000-4000 newborns worldwide, whereas it is much higher in  
62 Bangladesh [5-9]. 11 genes, including thyroid gland development and thyroid hormone  
63 biosynthesis, have been documented [10]. A defect in thyroid gland development due to mutations  
64 in both gene alleles of the pathway is known as thyroid dysgenesis. In contrast, a defect in thyroid  
65 hormone biosynthesis due to mutations in both alleles of a gene of the pathway is called thyroid  
66 dyshormonogenesis (TDH). TDH occurs due to mutations commonly found in seven genes,  
67 including TPO as a significant contributor to them [11, 12]. Since thyroid hormones are iodinated,  
68 TPO catalyzes the iodination steps, and mutations in the TPO gene may cause either total iodide  
69 organification defect (TIOD) or partial iodine organification defect (PIOD). Different countries  
70 conducted several studies on screening and identification of mutations in the TPO gene causing  
71 TIOD and PIOD [13-18]. Our previous study investigated that only genetic causes accounted for  
72 all of the CH patients with dyshormonogenesis in hospital settings in Bangladesh and didn't find  
73 any other aetiology [19]. Since CH is easily treatable, it is important to investigate the aetiology,  
74 which would help to determine how long the patients need hormone replacement therapy. The CH  
75 patients with genetic aetiology need lifelong hormone therapy [20]. Sometimes, neonatal CH  
76 screening using biochemical tests becomes difficult due to the presence of maternal TSH in the  
77 specimens of neonates, and this problem can be overcome by genetic screening at an early age  
78 [20]. There is limited data on investigating the genetic causes of CH in Bangladesh. However, we  
79 have performed several genetic studies and found mutations in patients with thyroid  
80 dyshormonogenesis [21] and thyroid dysgenesis [22].

81 High-resolution melting (HRM) curve analysis is one of the molecular tests, which is a high  
82 throughput real-time PCR technique based on the melting properties of double-stranded DNA.  
83 HRM can differentiate genetic variations such as homozygous or heterozygous states for specific  
84 mutations compared to the wild-type state in various genetic diseases, including autosomal  
85 recessive, autosomal dominant, and X-linked recessive disorders [23-26].

86 This study aimed to establish HRM curve analysis as a supplementary screening approach of  
87 Sanger sequencing targeting three common mutations in Bangladeshi patients. It could play an  
88 essential role in screening mass populations since it is faster, cheaper, and more reliable to detect  
89 genetic variations for improving the dimensions of newborn screening, which is neglected in  
90 Bangladeshi children.

91

## 92 **2. Methods and Materials**

### 93 **2.1. Study participant enrolment and specimen collection**

94 We enrolled a total of 36 confirmed cases of congenital hypothyroid children with  
95 dyshormonogenesis confirmed by an ultrasonogram of the thyroid gland in the clinical settings of  
96 the National Institute of Nuclear Medicine and Allied Sciences (NINMAS) and Department of  
97 Endocrinology, Bangabandhu Sheikh Mujib Medical University (BSMMU), Dhaka, Bangladesh.

98

### 99 **2.2. Ethics approval and consent to participate**

100 This study was approved by the Ethical Review Board for Human Studies of BSMMU and the  
101 Human Participants Committee, University of Dhaka (CP-4029) on 16 May 2017. After obtaining  
102 the ethical approval, we enrolled patients and collected their specimens from 1 June 2017 to 31  
103 December 2019. Blood specimens were collected from the participants with informed written  
104 consent from their parents or guardians.

105

### 106 **2.3. Laboratory investigation**

#### 107 **2.3.1. DNA isolation, PCR amplification, and Sanger Sequencing**

108 Blood specimens (3 mL) were collected, and genomic DNA was isolated using the QIAGEN  
109 FlexiGene® DNA Kit, followed by PCR and Sequencing [19]. After that, 20 pre-sequenced  
110 specimens were subjected to HRM, and then 16 unknowns were tested.

111

#### 112 **2.3.2. Method setup and validation of High-Resolution Melt curve analysis**

113 For analysis of *TPO* gene mutations by HRM method, we targeted three nonsynonymous  
114 mutations in the *TPO* gene identified by Sanger sequencing. For this purpose, we designed three  
115 sets of primers for detecting c.1117G>T and c.1193G>C mutations in exon eight and c.2173A>C  
116 mutation in exon 12. The primer sequences are listed in Table 1. First of all, those mentioned  
117 above, 20 pre-sequenced specimens with known mutations were used as reference samples to set  
118 up the HRM method. Homozygous, heterozygous, and wild-type specimens for the specific  
119 mutations were subjected to HRM curve analysis. Finally, 16 unknown samples were run to  
120 validate the method. These 16 samples were further tested by Sanger sequencing to confirm the  
121 mutation and validate the HRM approach.

122 **Table 1: List of primers used in HRM curve analysis**

Primer name	Mutation (nucleotide position)	Primer sequences (5'-3')	Product size (base pair)
TPO_G1117T_Ex8	c.1117G>T	Forward: CGCCTACCTGCCCTTCGTGC	101
		Reverse: CGTCTCCGGCCAGGAAGCAG	
TPO_G1193C_Ex8	c.1193G>C	Forward: CTGCTTCCTGGCCGGAGACG	65
		Reverse: ACAGCGTGTGCAGTGCCGTCAG	
TPO_A2173C_Ex12	c.2173A>C	Forward: AGACTTTGAGTCTTGTGACAGC	90
		Reverse: GTGAGAGGAGACCGAACTTCACC	

123  
124 To amplify the target sequence, a master mix was prepared following the protocol provided with  
125 the Precision Melt Supermix kit (Bio-Rad). To a reaction mixture of 5  $\mu$ L of 2X precision melt  
126 super mix, 0.2  $\mu$ L of each forward and reverse primer and 1  $\mu$ L of DNA (50 ng); 3.6  $\mu$ L nuclease-  
127 free water were added to make the reaction volume up to 10  $\mu$ L. Moreover, for detection of  
128 c.1193G>C mutation by HRM, 8mM MgCl<sub>2</sub> was added to the reaction mixture, and the reaction  
129 volume was adjusted accordingly. The cyclic condition was divided into two steps, namely real-  
130 time PCR amplification followed by melt curve analysis using a single program. The real-time  
131 PCR-based HRM was performed on a CFX96 Touch™ Real-Time PCR machine (Bio-Rad). The  
132 real-time PCR cyclic condition was as follows: initial denaturation at 95°C for 3 min; 40 cycles of  
133 denaturation at 95°C for 10 s, annealing at 60°C for 15 s and extension at 72°C for 15 s. After

134 completion of the real-time PCR, the subsequent melt curve program was initiated through cycles  
135 of denaturation at 95°C for 30 s, renaturation at 60°C for 1 min, and then melting at 65°C to 95°C  
136 with an increment of 0.1°C per 5 s for c.1117G>T and c.2173A>C mutations. And notably, an  
137 increment of 0.2°C per 5 s was used for c.1193G>C mutation. After completion of the real-time  
138 PCR-HRM, the data were analyzed using Precision Melt Analysis™ Software (BioRad). The melt  
139 curve shape sensitivity for cluster detection was set to 100%. The difference in the  $T_m$  threshold  
140 for the cluster detection was set to 0.1 to 0.2, and the normalized and temperature-shifted views  
141 were used for analysis. The results of pre-sequenced samples were compared with HRM analysis,  
142 and an additional 16 unknown samples were subjected to validate the HRM method using the same  
143 procedure that was followed for the pre-sequenced known samples. Finally, the normalized melt  
144 curve and the difference curves for both wild-type and mutant specimens (homozygous and  
145 heterozygous) were calculated and analyzed to detect the mutations in the *TPO* gene.

146

### 147 **3. Results**

148 Among 36 participants, 21 (58.33%) were males, and 15 (41.67%) were females. The average age  
149 of the participants was 7.97±4.29 (years) mean± SD, and the BMI was 17.0±4.4 (Kg/m<sup>2</sup>) mean±  
150 SD.

#### 151 **3.1. Screening of c.1117G>T mutation using HRM analysis**

152 To establish a rapid HRM-based screening approach targeting the c.1117G>T variant, a pair of  
153 primers (TPO\_G1117T\_Ex8) was designed that flanked the c.1117G>T variant. Then, the pre-  
154 genotyped samples were subjected to real-time PCR followed by HRM analysis. The fluorescence  
155 started to drop quickly at the initial melting phase for heterozygous samples. However, in the later  
156 phase of melting, the homozygous samples started to lose fluorescence intensity quicker than the  
157 heterozygous samples, and as a consequence, they crossed each other at a certain point of melting,  
158 making them distinguishable from each other. Similar to the normalized melting curve (Fig 1), the  
159 temperature-shifted difference curve could generate distinctive melting patterns for the wild-type,  
160 homozygous and heterozygous specimens (Fig 2). The reliability of the method was further  
161 validated by analyzing 16 unknown samples with dysgonadotropinemia. At first, these samples were  
162 tested by HRM, and then Sanger sequencing was done to check the sensitivity and specificity of  
163 the method. A total of 5 specimens had c.1117G>T variant in heterozygous states, six specimens

164 were in a homozygous state, and the remaining 5 had the wild type allele. The HRM result was  
165 consistent with the sequencing data, implying that sensitivity and specificity for detecting the  
166 c.1117G>T variant was 100% for both homozygous and heterozygous alleles.

167 **Fig 1.** Normalized melt curves for the specimens targeting the c.1117G>T variant in exon-8.

168 Normalized melt curves showing that the specimens with homozygous and heterozygous states are clearly  
169 distinguishable from the wild-type specimens, as manifested by the difference in relative fluorescence unit.

170

171 **Fig 2.** Difference curves generated by specimens targeting the c.1117G>T variant in exon-8. Discernable changes in  
172 three difference curves were showing that the specimens with homozygous and heterozygous states are clearly  
173 distinguishable from the wild type allele, as manifested by the difference in relative fluorescence unit.

174

### 175 **3.2. Screening of c.1193G>C mutation using HRM analysis**

176 The second set of primers, namely TPO\_G1193C\_Ex8, was used for the analysis of the c.1193G>C  
177 variant by the HRM approach. When the pre-genotyped samples were subjected to HRM analysis,  
178 three different clusters were observed in the melt curve analysis. One of the clusters corresponded  
179 to the heterozygous samples; the other two were for the homozygous samples and for the wild-  
180 type samples (Fig 3). However, in the difference curve analysis, three different clusters were  
181 clearly observed for homozygous, heterozygous, and wild-type variants of c.1193G>C (Fig 4). A  
182 similar observation was observed with 16 unknown samples that were subjected to HRM analysis.  
183 Four out of 16 samples came out as heterozygous by HRM analysis, and this result was consistent  
184 with the sequencing data. However, eight homozygous and four wild-type samples formed  
185 different clusters in this case. This observation implies that both heterozygous and homozygous  
186 states for c.1193G>C variant could be detected with 100% sensitivity and specificity.

187 **Fig 3.** Normalized melt curves generated by specimens targeting the c.1193G>C variant in exon-8. Discernable  
188 changes in normalized melt curves were showing that the specimens with homozygous (orange color) and  
189 heterozygous (green color) states are clearly distinguishable from the wild type (purple color) alleles, as manifested  
190 by the difference in relative fluorescence unit.

191 **Fig 4.** Difference curves for specimens targeting the c.1193G>C variant in exon-8. Discernable changes in difference  
192 curves were showing that the specimens with homozygous and heterozygous states are clearly distinguishable from  
193 the wild-type states, as manifested by the difference in relative fluorescence unit.

194

### 195 **3.3. Screening of c.2173A>C mutation using HRM analysis**

196 The third set of primers, namely TPO\_A2173C\_Ex12, was used to analyze another TPO gene  
197 mutation designated as c.2173A>C. The pre-genotyped wild type, homozygous c.2173A>C, and  
198 heterozygous c.2173A>C specimens were subjected to HRM analysis. The wild type, homozygous  
199 and heterozygous variants formed distinct clusters (Fig 5 and Fig 6). The homozygous c.2173A>C  
200 substitution resulted in an increase in melting temperature, and thus, the specimens with  
201 homozygous c.2173A>C variant had higher fluorescence intensity than that with the wild-type  
202 allele during melting, as manifested by the relative fluorescence unit (Fig 5). On the other hand,  
203 although the specimens with the heterozygous c.2173A>C variant followed a melting pattern with  
204 lower fluorescence intensity initially compared to the wild type, and the melting curve patterns  
205 almost overlapped with each other in a later stage (upper panel of Fig 5). Thus, homozygous  
206 c.2173A>C, heterozygous c.2173A>C, and the wild-type alleles were discernable from each other.  
207 Similar to the normalized melting curve, the difference curve analysis could also distinguish  
208 different states involving the c.2173A>C variant (Fig 6). HRM analysis of 16 unknown samples  
209 targeting the c.2173A>C variant was also 100% sensitive and specific. The HRM approach showed  
210 that 5 out of 16 unknown samples were wild type, 6 were homozygous, and the rest 5 were  
211 heterozygous. Sequencing of those 16 unknown samples revealed that the PCR HRM-based result  
212 was consistent with the sequencing result.

213 **Fig 5.** Normalized melt curves for specimens targeting the c.2173A>C variant in exon-12. Discernable changes in  
214 normalized melt curves were showing that the specimens with homozygous and heterozygous states are clearly  
215 distinguishable from the wild-type alleles, as manifested by the difference in relative fluorescence unit.

216 **Fig 6.** Differential curves for specimens targeting the c.2173A>C variant in exon-12. Discernable changes in  
217 difference curves showing specimens with homozygous and heterozygous states are clearly distinguishable from the  
218 wild type, as manifested by the difference in relative fluorescence unit.

219

## 220 **4. Discussion**

221 Congenital hypothyroidism (CH) is the most common cause of intellectual disabilities in children  
222 [27]. If early detection of CH is performed and treatment is initiated within 28 days of birth, clinical  
223 complications can be reversed by treatment with Levothyroxine, which is very easy to administer



224 and affordable. Although 11 genes have been reported to be responsible for all CH cases with  
225 genetic aetiology, only seven genes are responsible for thyroid dyshormonogenesis, and published  
226 data have suggested that one of the major genes for thyroid dyshormonogenesis is thyroid  
227 peroxidase (TPO), and its mutations are inherited in an autosomal recessive manner to cause the  
228 disease [13, 28, 29]. TPO enzyme catalyzes the iodine oxidation process in the thyroid hormone  
229 synthesis pathway [30]. To date, approximately 60 mutations in the *TPO* gene have been reported  
230 in a total of 17 exons in the *TPO* gene [14, 31-33]. Global publications on the *TPO* gene in  
231 hypothyroid patients demonstrated that most of the mutations were confined between exon 7 and  
232 exon 14, and very few mutations had been identified outside this region [32][34]. Although the  
233 mutations had been detected as homozygous or heterozygous states, our study confirmed that both  
234 alleles of the *TPO* gene of all 36 hypothyroid patients had been affected by mutations, further  
235 confirming the recessive pattern of this disease. The identified nonsynonymous mutations had  
236 previously been reported to be pathogenic or disease-causing mutations [12, 18].

237 A genetic study investigated that mutation c.1117G>T and c.2173A>C showed a non-enzymatic  
238 reaction rate, and mutation c.1193G>C showed a slightly reduced enzymatic reaction rate  
239 compared to the wild-type TPO protein [34]. Our previous study identified four common mutations  
240 in the hotspot region from exon 8 to exon 12 in the TPO gene and studied their effect on the 3D  
241 structure of the TPO protein [19]. Since we found these common mutations in Bangladeshi  
242 patients, we aimed to establish an alternative method of Sanger sequencing to screen the patients.  
243 In Bangladesh, there is very little information about newborn screening and the genetic aetiology  
244 of CH. High-resolution melting (HRM) methodology represents a significant advancement in  
245 mutation detection over the years. The HRM method has been established for the detection of  
246 variants of the beta-globin gene in thalassemia patients and G6PD deficiency in Bangladesh [24,  
247 35].

248 The genetic study is important to investigate the cause of CH. There are some screening methods  
249 for the diagnosis of CH, such as measurement of serum/blood TSH, T3, and T4. However, these  
250 approaches can only confirm the CH cases but not the actual aetiology. That is, the conventional  
251 screening method for CH cannot say whether it is acquired or genetic. If the actual aetiology is  
252 known, the duration of treatment can be defined based on the causes. If it is due to a genetic cause,  
253 the patients could be enrolled for levothyroxine treatment for their whole life. On the other hand,  
254 treatment should be continued for the first three years of life for an acquired cause [20]. So, the

255 treatment strategy will be different for CH cases with genetic aetiology and other reasons for CH  
256 with dys hormonogenesis. If the genetic basis of CH is defined in the country, carrier screening is  
257 possible to target the underlying genetic cause. If the parents are found to be carriers of CH  
258 involving the TPO gene, their children or newborns could be screened, and appropriate measures  
259 can be taken, such as early initiation of treatment, which would help to prevent mental retardation.  
260 Late diagnosis of CH is common in our country, and an initial pilot study suggested that late-  
261 diagnosed hypothyroid children had clinical complications even under levothyroxine treatment in  
262 Bangladesh. So newborn screening should be a common practice for early CH diagnosis to prevent  
263 mental retardation due to late diagnosis.

264 The present study aimed to establish HRM-targeted mutations c.1117G>T, c.1193G>C, and  
265 c.2173A>C commonly found in Bangladeshi patients. To validate the method, we designed  
266 primers covering the mutational hotspot, keeping the product size between 65-101 base pairs,  
267 which fulfilled the requirement of the HRM strategy [36]. To establish HRM, the samples with  
268 heterozygous, homozygous, and wild-type alleles were subjected to an experiment. For the first  
269 set of primers targeted the mutation c.1117G>T, both homozygous and heterozygous states were  
270 clearly distinguishable from wild-type alleles. However, c.1193G>C mutation was much more  
271 difficult to differentiate due to the formation of a similar number of hydrogen bonds for G>C  
272 substitution, and thus similar level bond energy was involved for both the wild type and mutant  
273 variants. To overcome these difficulties, the optimum concentration of MgCl<sub>2</sub> was determined to  
274 be 8 mM for detection of a single G>C point mutation by HRM because 8 mM MgCl<sub>2</sub>  
275 concentration could clearly distinguish among homozygous, heterozygous, and wild-type alleles.  
276 This showed that MgCl<sub>2</sub> could have an effect on HRM studies to differentiate different states of  
277 mutation of G/C alleles. For the c.1193G>C mutation, the melt curve showed almost similar  
278 patterns among the samples with the wild-type allele and also samples with homozygous and  
279 heterozygous alleles. However, the temperature-shifted curve could clearly differentiate all the  
280 states. Different studies demonstrated that the HRM method could not distinguish purine to  
281 pyrimidine nucleotide substitution, such as A to T or G to C substitution, due to the same melting  
282 temperature [36-38]. For the third mutation, c.2173A>C, Adenine nucleotide was substituted by  
283 Cytosine nucleotide, and due to the difference in bond energy between Purine and pyrimidine  
284 group, the melting temperature was shifted for both heterozygous and homozygous states  
285 compared to the wild type state. The temperature-shifted pattern was differentiated in such a

286 manner that the wild type had a lower T<sub>m</sub> pattern compared to the heterozygous and homozygous  
287 states.

288 Although Sanger sequencing is the gold standard for mutation detection, HRM can be used as a  
289 fast and less expensive supplemental approach with 100% sensitivity and specificity for screening  
290 and detection of mutations in the TPO gene in Bangladeshi patients. Since TPO gene mutation is  
291 inherited in an autosomal recessive manner to cause dysmorphogenesis, this HRM method can  
292 also investigate its carrier state.

293

## 294 **5. Conclusion**

295 High-resolution melt curve analysis could be an alternative approach for screening common  
296 mutations in the *TPO* gene in Bangladeshi patients with thyroid dysmorphogenesis so that  
297 complications of late-diagnosed patients can be prevented by early screening and initiation of  
298 treatment in a different strategy.

299

## 300 **Acknowledgements**

301 The authors are thankful to University Grants Commission (UGC) of Bangladesh for its  
302 generous support.

303

## 304 **References**

- 305 1. Rastogi MV, LaFranchi SH. Congenital hypothyroidism. *Orphanet journal of rare diseases*.  
306 2010;5(1):17.
- 307 2. Razavi Z, Mohammadi L. Permanent and transient congenital hypothyroidism in Hamadan West  
308 Province of Iran. *International journal of endocrinology and metabolism*. 2016;14(4).
- 309 3. Grüters A, Krude H. Detection and treatment of congenital hypothyroidism. *Nature Reviews*  
310 *Endocrinology*. 2012;8(2):104.
- 311 4. LaFranchi SH, Austin J. How should we be treating children with congenital hypothyroidism?  
312 *Journal of Pediatric Endocrinology and Metabolism*. 2007;20(5):559-78.
- 313 5. Klett M. Epidemiology of congenital hypothyroidism. *Experimental and Clinical Endocrinology &*  
314 *Diabetes*. 1997;105(S 04):19-23.
- 315 6. Harris KB, Pass KA. Increase in congenital hypothyroidism in New York State and in the United  
316 States. *Molecular genetics and metabolism*. 2007;91(3):268-77.
- 317 7. Deladoëy J, Bélanger N, Van Vliet G. Random variability in congenital hypothyroidism from thyroid  
318 dysgenesis over 16 years in Quebec. *The Journal of Clinical Endocrinology & Metabolism*. 2007;92(8):3158-  
319 61.

- 320 8. Olney RS, Grosse SD, Vogt RF. Prevalence of congenital hypothyroidism—current trends and  
321 future directions: workshop summary. *Pediatrics*. 2010;125(Supplement 2):S31-S6.
- 322 9. Hasan M, Nahar N, Ahmed A, Moslem F. Screening for congenital hypothyroidism—a new era in  
323 Bangladesh. *SOUTHEAST ASIAN JOURNAL OF TROPICAL MEDICINE AND PUBLIC HEALTH*. 2004;34:162-4.
- 324 10. Park S, Chatterjee V. Genetics of congenital hypothyroidism. *Journal of medical genetics*.  
325 2005;42(5):379-89.
- 326 11. Grasberger H, Refetoff S. Genetic causes of congenital hypothyroidism due to  
327 dysmorphogenesis. *Current opinion in pediatrics*. 2011;23(4):421.
- 328 12. Avbelj M, Tahirovic H, Debeljak M, Kusekova M, Toromanovic A, Krzisnik C, et al. High prevalence  
329 of thyroid peroxidase gene mutations in patients with thyroid dysmorphogenesis. *European journal of*  
330 *endocrinology*. 2007;156(5):511-9.
- 331 13. Rivolta CM, Esperante SA, Gruñeiro-Papendieck L, Chiesa A, Moya CM, Domené S, et al. Five novel  
332 inactivating mutations in the thyroid peroxidase gene responsible for congenital goiter and iodide  
333 organification defect. *Human mutation*. 2003;22(3):259-.
- 334 14. Bakker B, Bikker H, Vulmsa T, de Randamie JS, Wiedijk BM, de Vijlder JJ. Two decades of screening  
335 for congenital hypothyroidism in The Netherlands: TPO gene mutations in total iodide organification  
336 defects (an update). *The Journal of Clinical Endocrinology & Metabolism*. 2000;85(10):3708-12.
- 337 15. Kotani T, Umeki K, Kawano Ji, Suganuma T, Hishinuma A, Ieiri T, et al. Partial iodide organification  
338 defect caused by a novel mutation of the thyroid peroxidase gene in three siblings. *Clinical endocrinology*.  
339 2003;59(2):198-206.
- 340 16. Rodrigues C, Jorge P, Soares JP, Santos I, Salomao R, Madeira M, et al. Mutation screening of the  
341 thyroid peroxidase gene in a cohort of 55 Portuguese patients with congenital hypothyroidism. *European*  
342 *Journal of Endocrinology*. 2005;152(2):193-8.
- 343 17. Wu J, Shu S, Yang C, Lee C, Tsai F. Mutation analysis of thyroid peroxidase gene in Chinese patients  
344 with total iodide organification defect: identification of five novel mutations. *Journal of Endocrinology*.  
345 2002;172(3):627-35.
- 346 18. Balmiki N, Bankura B, Guria S, Das TK, Pattanayak AK, Sinha A, et al. Genetic analysis of thyroid  
347 peroxidase (TPO) gene in patients whose hypothyroidism was found in adulthood in West Bengal, India.  
348 *Endocrine journal*. 2014;61(3):289-96.
- 349 19. Begum M, Islam MT, Hossain SR, Bhuyan GS, Halim MA, Shahriar I, et al. Mutation spectrum in  
350 TPO gene of Bangladeshi patients with thyroid dysmorphogenesis and analysis of the effects of different  
351 mutations on the structural features and functions of TPO protein through in silico approach. 2019;2019.
- 352 20. Büyükgebiz A. Newborn screening for congenital hypothyroidism. *Journal of Pediatric*  
353 *Endocrinology and Metabolism*. 2006;19(11):1291-8.
- 354 21. Begum MN, Mahtarin R, Ahmed S, Shahriar I, Hossain SR, Mia MW, et al. Investigation of the  
355 impact of nonsynonymous mutations on thyroid peroxidase dimer. 2023;18(9):e0291386.
- 356 22. Begum MN, Mahtarin R, Islam MT, Ahmed S, Konika TK, Mannoor K, et al. Molecular investigation  
357 of TSHR gene in Bangladeshi congenital hypothyroid patients. 2023;18(8):e0282553.
- 358 23. Yan J-b, Xu H-p, Xiong C, Ren Z-r, Tian G-l, Zeng F, et al. Rapid and reliable detection of glucose-6-  
359 phosphate dehydrogenase (G6PD) gene mutations in Han Chinese using high-resolution melting analysis.  
360 *The Journal of Molecular Diagnostics*. 2010;12(3):305-11.
- 361 24. Islam MT, Sarkar SK, Sultana N, Begum MN, Bhuyan GS, Talukder S, et al. High resolution melting  
362 curve analysis targeting the HBB gene mutational hot-spot offers a reliable screening approach for all  
363 common as well as most of the rare beta-globin gene mutations in Bangladesh. *BMC genetics*.  
364 2018;19(1):1.
- 365 25. Bono C, Nuzzo D, Albeggiani G, Zizzo C, Francofonte D, Iemolo F, et al. Genetic screening of Fabry  
366 patients with EcoTILLING and HRM technology. *BMC research notes*. 2011;4(1):323.

- 367 26. Bataille S, Berland Y, Fontes M, Burtsey S. High Resolution Melt analysis for mutation screening in  
368 PKD1 and PKD2. *BMC nephrology*. 2011;12(1):57.
- 369 27. Grosse SD, Van Vliet G. Prevention of intellectual disability through screening for congenital  
370 hypothyroidism: how much and at what level? *Archives of disease in childhood*. 2011:archdischild190280.
- 371 28. Pannain S, Weiss RE, Jackson CE, Dian D, Beck JC, Sheffield VC, et al. Two different mutations in  
372 the thyroid peroxidase gene of a large inbred Amish kindred: power and limits of homozygosity mapping.  
373 *The Journal of Clinical Endocrinology & Metabolism*. 1999;84(3):1061-71.
- 374 29. Fugazzola L, Mannavola D, Vigone MC, Cirello V, Weber G, Beck-Peccoz P, et al. Total iodide  
375 organification defect: clinical and molecular characterization of an Italian family. *Thyroid*.  
376 2005;15(9):1085-8.
- 377 30. Taurog A, Dorris M, Doerge DR. Evidence for a radical mechanism in peroxidase-catalyzed  
378 coupling. I. Steady-state experiments with various peroxidases. *Archives of biochemistry and biophysics*.  
379 1994;315(1):82-9.
- 380 31. Belforte FS, Miras MB, Olcese MC, Sobrero G, Testa G, Muñoz L, et al. Congenital goitrous  
381 hypothyroidism: mutation analysis in the thyroid peroxidase gene. *Clinical endocrinology*. 2012;76(4):568-  
382 76.
- 383 32. Bikker H, Vulsma T, Baas F, de Vijlder JJ. Identification of five novel inactivating mutations in the  
384 human thyroid peroxidase gene by denaturing gradient gel electrophoresis. *Human Mutation*.  
385 1995;6(1):9-16.
- 386 33. Kimura S, Hong YS, Kotani T, Ohtaki S, Kikkawa F. Structure of the human thyroid peroxidase gene:  
387 comparison and relationship to the human myeloperoxidase gene. *Biochemistry*. 1989;28(10):4481-9.
- 388 34. Guria S, Bankura B, Balmiki N, Pattanayak AK, Das TK, Sinha A, et al. Functional analysis of thyroid  
389 peroxidase gene mutations detected in patients with thyroid dysmorphogenesis. *International journal*  
390 *of endocrinology*. 2014;2014.
- 391 35. Islam MT, Sarker SK, Talukder S, Bhuyan GS, Rahat A, Islam NN, et al. High resolution melting curve  
392 analysis enables rapid and reliable detection of G6PD variants in heterozygous females. *BMC genetics*.  
393 2018;19(1):58.
- 394 36. Stomka M, Sobalska-Kwapis M, Wachulec M, Bartosz G, Strapagiel D. High Resolution Melting  
395 (HRM) for High-Throughput Genotyping—Limitations and Caveats in Practical Case Studies. *International*  
396 *journal of molecular sciences*. 2017;18(11):2316.

397

## 398 **Supporting information**

399 **S1 Table. Sequenced samples that were used for the HRM method setup.**

400 **S2 Table. Unknown samples used for HRM method validation.**

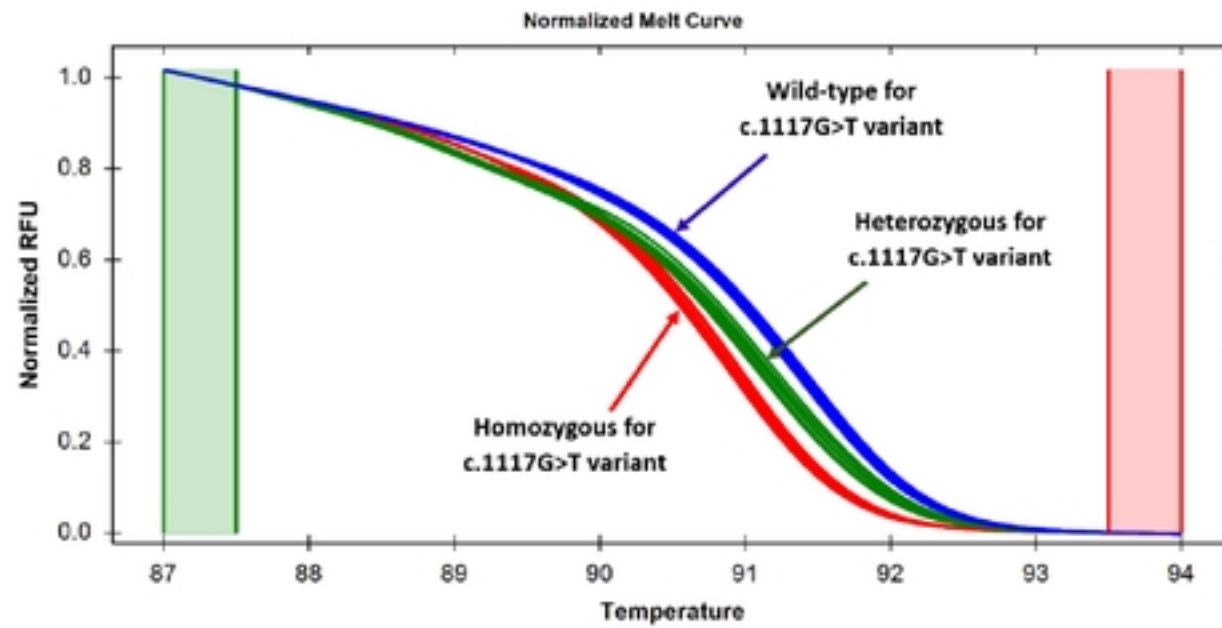


**Fig 1.** Normalized melt curves for the specimens targeting the c.1117G>T variant in exon-8. medRxiv preprint doi: <https://doi.org/10.1101/2023.10.17.23297147>; this version posted October 18, 2023. The copyright holder for this preprint (which was not certified by peer review) is the author/funder, who has granted medRxiv a license to display the preprint in perpetuity. It is made available under a [CC-BY 4.0 International license](https://creativecommons.org/licenses/by/4.0/).

Normalized melt curves showing that the specimens with homozygous and heterozygous states are clearly distinguishable from the wild-type specimens, as manifested by the difference in relative fluorescence unit.

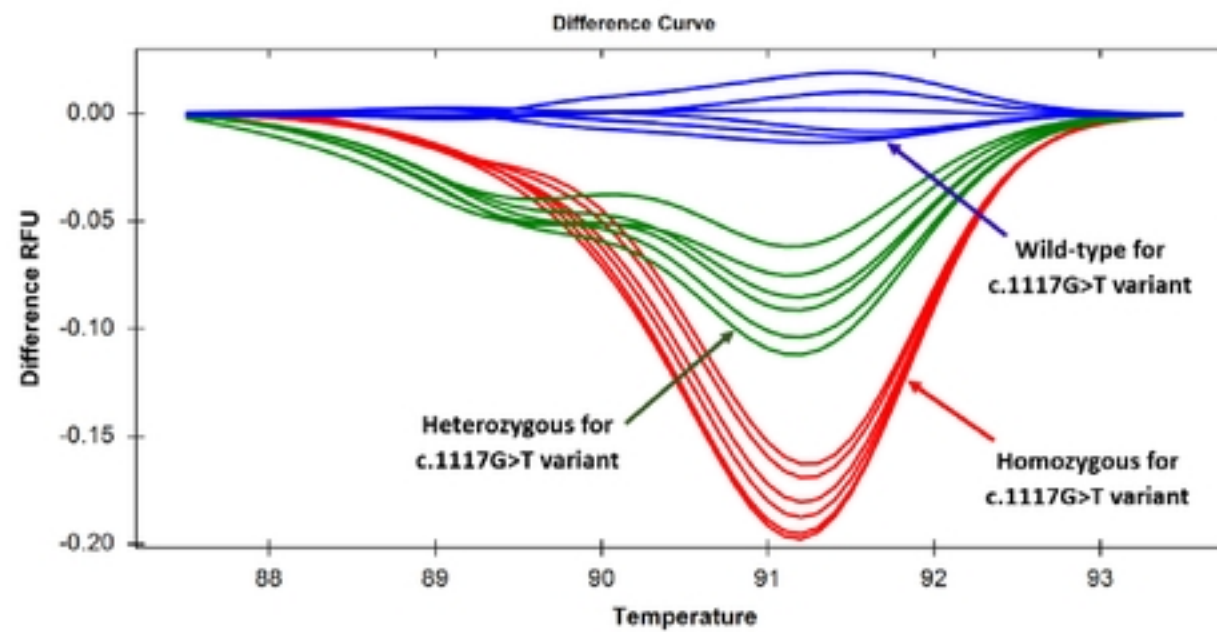


**Fig 2.** Difference curves generated by specimens targeting the c.1117G>T variant in exon-8. Discernable changes in three difference curves were showing that the specimens with homozygous and heterozygous states are clearly distinguishable from the wild type allele, as manifested by the difference in relative fluorescence unit.

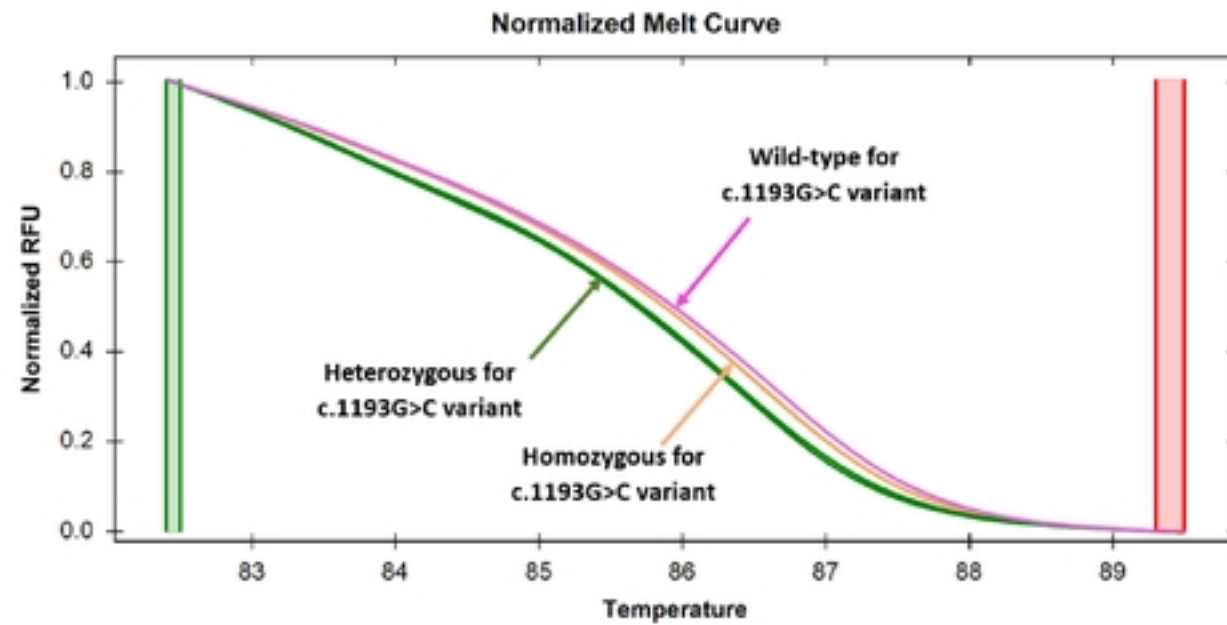


**Fig 3.** Normalized melt curves generated by specimens targeting the c.1193G>C variant in exon-8. Discernable changes in normalized melt curves were showing that the specimens with homozygous (orange color) and heterozygous (green color) states are clearly distinguishable from the wild type (purple color) alleles, as manifested by the difference in relative fluorescence unit.

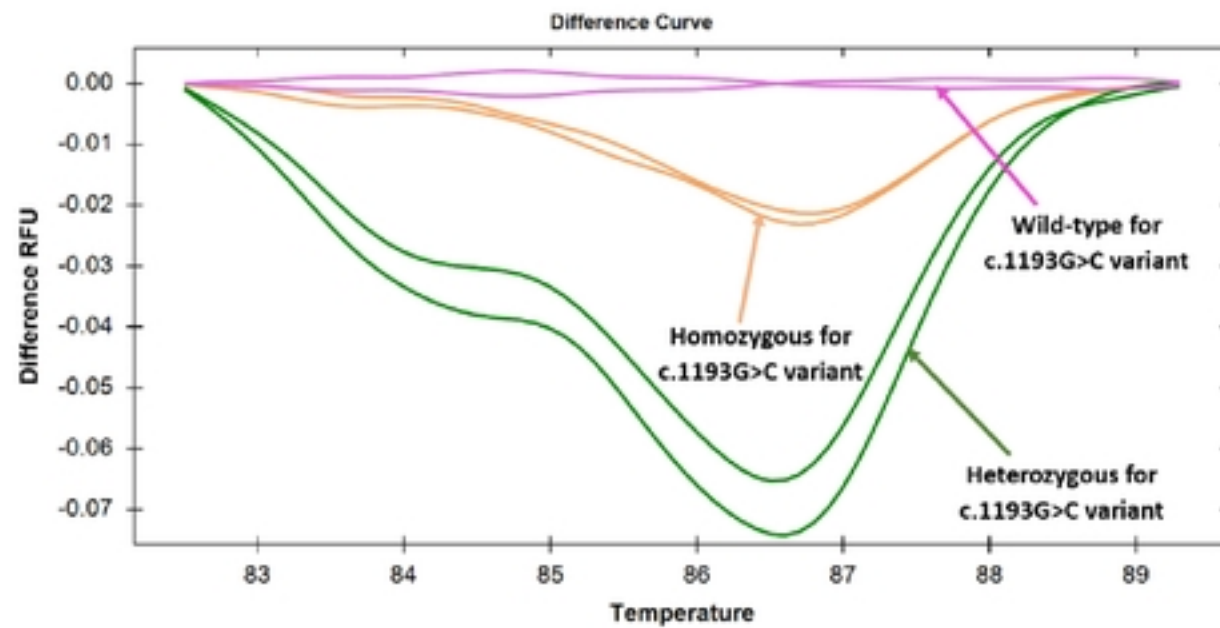
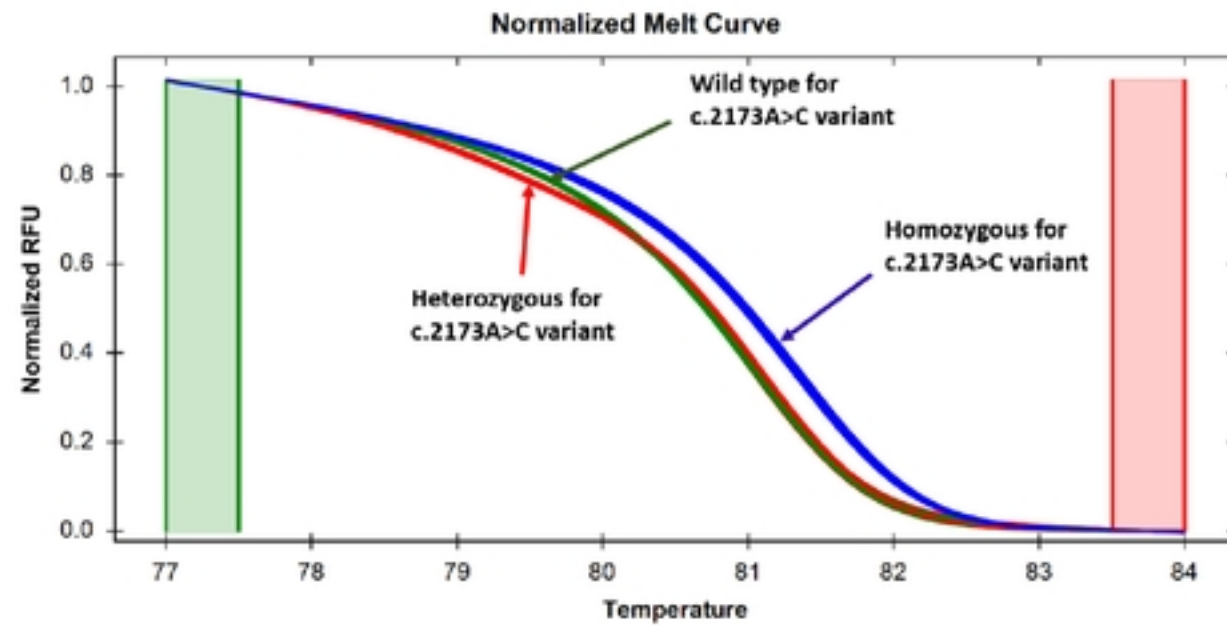


**Fig 4.** Difference curves for specimens targeting the c.1193G>C variant in exon-8. Discernable changes in difference curves were showing that the specimens with homozygous and heterozygous states are clearly distinguishable from the wild-type states, as manifested by the difference in relative fluorescence unit.



medRxiv preprint doi: <https://doi.org/10.1101/2023.10.17.23291147>; this version posted October 16, 2023. The copyright holder for this preprint (which was not certified by peer review) is the author/funder, who has granted medRxiv a license to display the preprint in perpetuity. It is made available under a [CC-BY 4.0 International license](https://creativecommons.org/licenses/by/4.0/).

Discernable changes in normalized melt curves were showing that the specimens with homozygous and heterozygous states are clearly distinguishable from the wild-type alleles, as manifested by the difference in relative fluorescence unit.

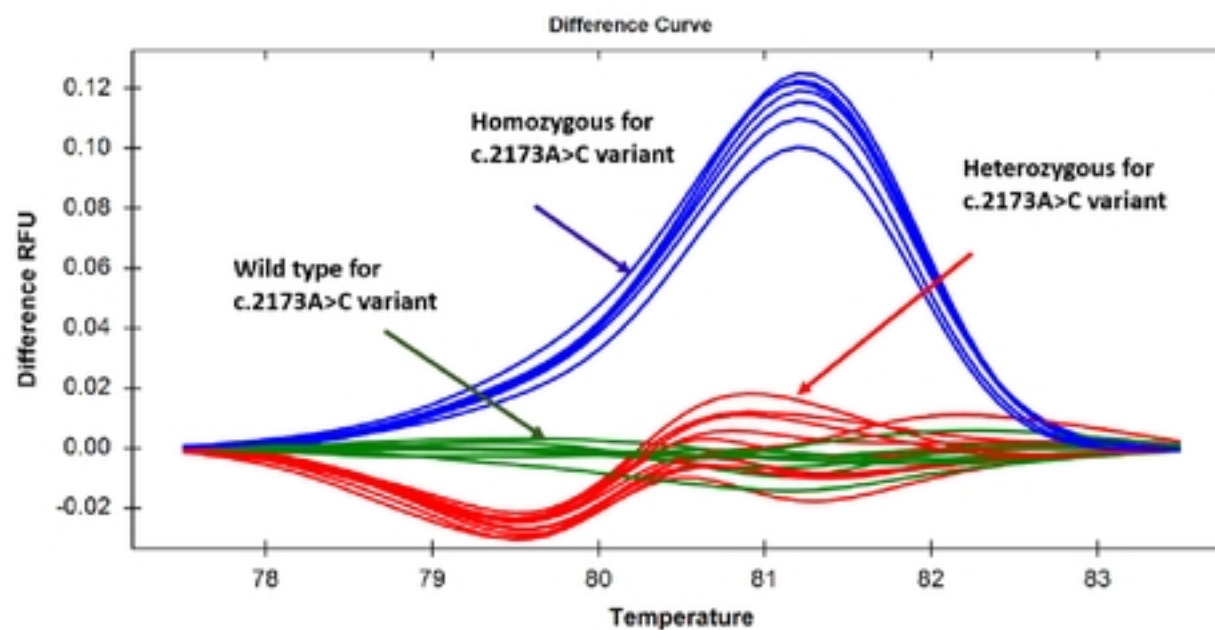


Fig 6. Differential curves for specimens targeting the c.2173A>C variant in exon-12. Discernable changes in difference curves showing specimens with homozygous and heterozygous states are clearly distinguishable from the wild type, as manifested by the difference in relative fluorescence unit.